International Journal Of Renewable Energy Research, IJRER
S.Tsotoulidis, A.Safacas, Vol.1, No3, pp.31-42 ,2011

Analysis of a Drive System in a Fuel Cell and Battery powered Electric Vehicle

Savvas Tsotoulidis*‡, Athanasios Safacas**

* Laboratory of Electromechanical Energy Conversion, Department of Electrical Engineer and Computer Science, University of Patras, Rio-Patras 26504, (*Greece*)

** Laboratory of Electromechanical Energy Conversion, Department of Electrical Engineer and Computer Science, University of Patras, Rio-Patras 26504, (*Greece*)

‡ Corresponding Author; University of Patras, Rio-Patras 26504, (*Greece*): Tel: +302610997351, Fax: +302610997362, e-mail: stsotoulidis@ece.upatras.gr, a.n.safacas@ece.upatras.gr

Received : 12.05.2011 Accepted : 13.06.2011

Abstract- In this paper the design and the operation of the drive system in a Fuel Cell Electric Vehicle (FCEV) is presented. The system consists of a Proton Exchange Membrane Fuel Cell (PEMFC) stack, an interleaved boost converter, battery pack connected via a bidirectional buck-boost converter and a brushless DC motor (BLDC) driven by a three phase inverter. A basic analysis of each component of the investigated system is presented. The main objective of this paper is to manage the energy transfer from the PEMFC stack to the DC bus based on wide high efficiency range. A battery pack is used for reducing the size of the stack and thus the cost, with by which regenerative braking is also achieved. In order to testify the nonlinear V-I characteristic curve of the PEMFC system experiments have been carried out. The performance of the overall system in steady state is studied via simulation in MATLAB/SIMULINK software. Two operating scenarios have been investigated. In the first, PEMFC stack and battery pack provide maximum power to the BLDC motor, while in the second, regenerative braking is accomplished via the bidirectional buck-boost converter to the battery pack by changing the control logic of the three phase inverter. Experiments have been carried out to validate the performance of the system at full load at steady state.

Keywords- PEM Fuel Cells, interleaved boost converter, drive system of electric vehicle, regenerative braking.

1. Introduction

Electric Vehicles (EVs), despite the relatively short period of time in which they possess a significant share of the automotive development, have already proven their value. In these vehicles, the challenges are to achieve high efficiency, low cost and small volume and mass [1]. Recent advances in FCs' technology create an increasing interest in using FCs for propulsion, onboard power generation and stationary power generation applications.

It is well known that FCs are electrochemical energy conversion devices which directly produce electricity, water and heat by processing hydrogen and oxygen. Therefore, pollution free electric power generation is accomplished if pure hydrogen is used, while low emissions are produced, when using other fuels, such as natural gas or methanol for the hydrogen production. An important feature of FCs is the high conversion efficiency during electrochemical process. Another advantage of FCs is their modularity, which makes them flexible to the production of voltage and current in different levels [2]. On the other hand, FCs have limitations on their dynamic response. Due to mechanical delays of the fuel delivery system such as valves and pumps and also the limited rate of heat release, the electrical time constants of a FC stack are relative high [3]. Therefore, an additional energy source is needed when rapid load variations

occur in order to improve system performance. This energy source could be an ultracapacitor or a battery pack.

For vehicle applications, the internal combustion engine (ICE) has lower total efficiency (*13.8%*) in respect to FC (*21.7%*) [4]. Also, the FC produces lower exhaust emissions and has lower operating noise in comparison to conventional ICEs [5]. Load requirements change during drive in vehicles and since FCs have a slow dynamic response, auxiliary energy source is needed as it was mentioned above. In our system an FC stack and a battery pack are included. This configuration has many advantages. The auxiliary energy storage device can supplement the FC Stack when the vehicle demands high power. As a result, FC Stack can be sized to cover a great rate of the maximum power and so the overall cost of the vehicle is reduced. Another advantage is the recovery of regenerative braking energy and the storage in the auxiliary source [6, 7].

The main drawback of a FCEV is the lack of availability of hydrogen which could be over by producing hydrogen from wind turbines and photovoltaic cells [8] or by reforming hydrocarbon such as natural gas.

In this work the configuration and the modeling of the drive system for a light FCEV are presented. The main energy source is provided by a PEMFC stack. Among several kinds of FCs, PEMFC has relatively high power density, smaller size, lower operating temperature and easy start.

In this work, the secondary energy source is a battery pack, which is connected to the DC bus via a suitable converter which will be described in the next section. Also regenerative braking is accomplished by using rechargeable batteries and a bidirectional buck – boost converter.

Analysis of the operation and performance of the FC – battery powered vehicle drive system has been done and it is assessed by simulation using MATLAB/SIMULINK software for two operating scenarios. In the first one, both FC and battery pack provide electrical energy to the BLDC motor, when full load is required. The rate of the energy provided by the FC must be such that the efficiency does not become lower than a defined rate (in our case it is 39%). At full load, the contribution of electric energy from both FC stack and battery pack is studied. In the second scenario, the BLDC machine operates as a generator storing energy in the battery pack, thus regenerative braking is accomplished and so the overall efficiency of the system can be increased. To avoid any current flow to the FC stack, a diode is connected in series to its output. Experimental work has been carried out to validate the system's performance.

2. System Description

The basic scheme of the system under investigation is shown in figure 1. It consists of a PEMFC stack, an interleaved boost converter with four legs, a battery pack with a bidirectional buck-boost converter to enable energy recovery in the case of regenerative braking, and a BLDC driven by a three phase inverter. The design of each component is discussed in the following.

A. PEMFC System

The PEMFC system included in the investigated structure is the Nexa Power Module – Ballard. It is composed of a FC stack, which converts pure hydrogen and air into electric energy, heat and water, and all the ancillary equipment necessary for the FC operation. The ancillary subsystems include hydrogen delivery, oxidant air supply and cooling air supply. The energy needed for the operation of these components is produced by the FC stack. The FC source's nominal power is *1200 W*, the nominal current is *48 A* and *44 V* is the open – circuit voltage.

The produced voltage by PEMFC stack depends on the temperature inside the cells, the inlet flow rate of Hydrogen, the inlet flow rate of Oxygen and the load current. The theoretical output voltage of a single PEMFC is *1.23 V*. The actual output voltage of a FC drops when current increases because of the overpotentials in electrodes and in membrane. It is described by the following sufficiently accurate equations [9]:

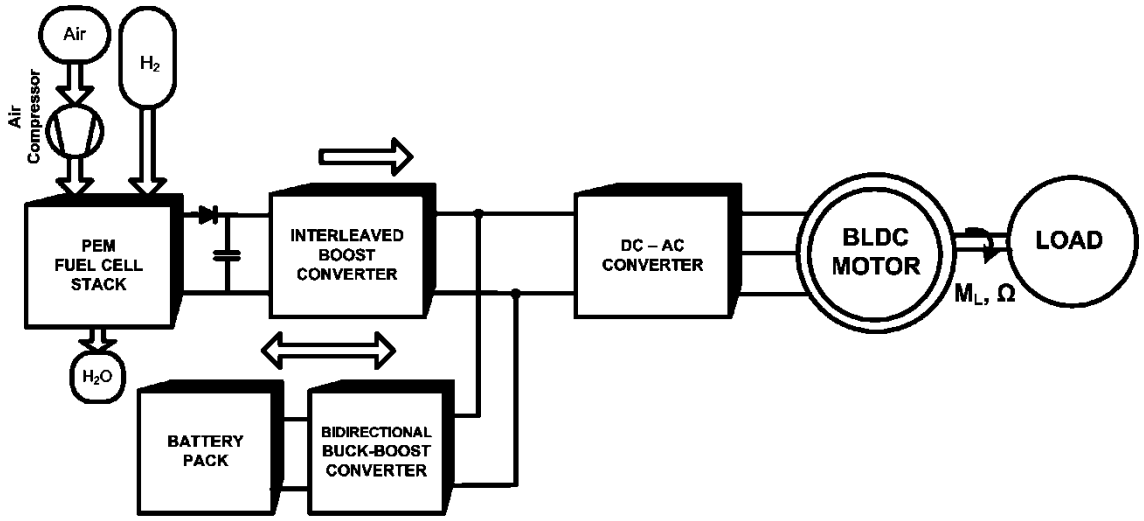

Fig.. 1. Basic structure of the investigated drive system in FCEV.

$$V_{cell} = E - E_{act} - E_{conc} - E_{ohmic} \quad (1)$$

where:

$$E_{act} = \frac{RT}{2\alpha F}\ln\left(\frac{i}{i_o}\right) \quad (2)$$

$$E_{conc} = \frac{RT}{2F}\ln\left(\frac{i_L}{i_L - i}\right) \quad (3)$$

$$E_{ohmic} = R_\Omega \cdot i, \quad (4)$$

The symbols in the previous equations have the following meaning: E represents the open-circuit voltage of a FC, E_{act} the voltage drop due to activation losses, E_{conc} the voltage drop due to concentration losses and E_{ohmic} the voltage drop due to ohmic losses. R stands for the ideal gas constant, T for the cell Temperature, F for the Faraday constant, i_O for reference exchange current density, i_L for limiting current density, R_Ω for ohmic resistance of the membrane and α for transfer coefficient.

To get higher operating voltage, FCs are connected in series and in case of having a FC stack consisting of N cells the voltage of the stack is given by following equation [9]:

$$V_{stack} = NV_{cell} = N\left(E - E_{act} - E_{conc} - E_{ohmic}\right) \quad (5)$$

The parameters of the above equations which have been used for the simulation model appear in Table 1.

Table 1. FC stack parameters [10]

R	$8.314\ Jmol^{-1}K^{-1}$
F	$96{,}485\ C.mol^{-1}$
i_o	$3*10^{-6}\ Acm^{-2}$
i_L	$2.5\ Acm^{-2}$
R_Ω	$0.25\ Ohmcm^2$
α	0.8
N	48

It is assumed that the temperature inside the cell is constant (T = 330^{o}K) since do not occur rapid load variations in the FC stack.

B. Interleaved boost converter with 4 legs

As it was mentioned above, the voltage produced by the stack is relative low. Therefore, a power electronic converter is needed to boost stack voltage to the required load voltage level, which is *50 V* in our case. The selection of the inductors' value (100μH for each leg) of the converter has been done to decrease the input current ripple. This

is a critical parameter for FC systems, which cannot cope to rapid and large variations of current due to starvation phenomena. Using a simple boost converter it leads to a large inductors' value with high volume and cost. Therefore an interleaved boost converter with *4* legs has been chosen in our investigation, as shown in figure 2.

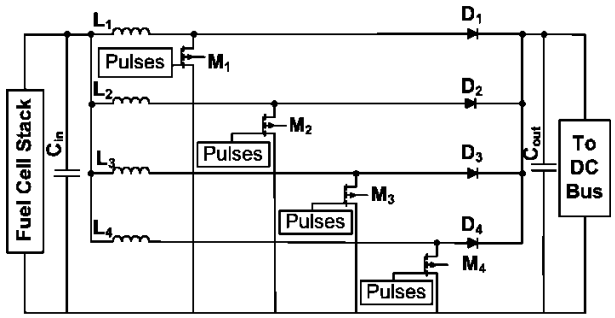

Fig. 2. Interleaved Boost Converter with 4 legs.

The main characteristic of this converter is that the legs conduct sequentially, with phase shift $360^o/N$ with each other, where N is the number of legs (in our case N = *4*). The main advantage of this converter is that the total current is equally shared to each leg and the conduction losses are reduced. However, the total switching losses increase, as we have more legs in the converter. The ripple of the input and of the output current, significally decreases compared to a single boost converter [2, 11].

STP30NF10 MOSFETs are used as power switches in the investigated interleaved boost converter. The switching frequency for the MOSFETs is *20 kHz*. Some of the main characteristics of these MOSFETs, provided by the manufacturer, are presented in Table 2

C. Batteries with a bidirectional buck-boost converter

The auxiliary system, enables recovery of regenerative braking energy and provides fast response and additional power during acceleration [12, 13], since FC has a slow transient response and limitations of the produced energy which depends on the fuel flow. Moreover, by using batteries to cover a rate of the energy demand, the size and therefore the cost of the FC stack is reduced. Finally, a more efficient operational behavior of the FC stack is achieved with an appropriate control strategy [14].

The battery pack has been sized so that it stores sufficient energy and provides adequate peak power for the vehicle to have a specified acceleration performance. It consists of two batteries of *12 V* each connected in series.

The secondary power source is connected to the dc bus via a bidirectional buck-boost converter. The schematic diagram of the converter is shown in figure 3. This converter has a rated power at *200W* in order to cover the max power of the BLDC motor. It can be pointed out that the structure of this converter differs from a conventional buck boost. The polarity of the input and output voltage is the same in its two operational modes.

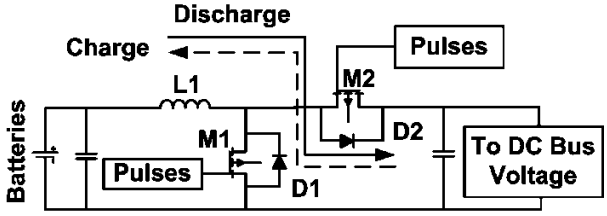

Fig. 3. Bidirectional Buck – Boost DC/DC converter.

Table 2. The main characteristics of STP30NF10

V_{ds}	max voltage between drain and source	*00 V*
I_d	max drain current at $T = 100^oC$	*5 A*
R_{ds}	max resistance between drain and source	*5 mΩ*
t_r+t_f	max rising and falling time delay	*10 ns*

During the boost phase, the battery pack voltage level of *24 V* is boosted to *48 V* and applied at the DC bus. On the other hand, during buck phase the generators' output voltage is regulated to the desirable level to recharge the batteries. The value of the DC bus voltage is used as criterion for changing the operation mode. When the DC bus voltage exceeds *55 V*, the buck mode is accomplished.

D. BLDC motor driven by a three phase inverter

A three phase BLDC motor with trapezoidal back Electromagnetic Force (EMF) is used in the investigated drive system, as shown in figure 4. The magnetic field of this motor is uniformly distributed in the air gap. With machine running at constant speed, this results in a back EMF which has a trapezoidal shape in time. The modulated technique has to ensure that the switching action is synchronized to the rotation of the flux in the air gap, and so the machine must have a sensor for measuring the position of the flux wave relative to that of the stator windings. Hall sensors are mounted symmetrical at 120^o electrical degree intervals, via which the position of the rotor can be known at any instance [15, 16].

The BLDC motor has a rated power of *1400 W* and operates by a supply voltage of *48 V* in the DC bus. Power is drawn from the DC bus by a three phase inverter driving the motor, where the switching of the power electronic elements is based on sensor feedback signals. It is well-known that the current fed to this motor must have a rectangular waveform. The parameters of the investigated BLDC motor are shown in Table 3.

Table 3. Parameters of the BLDC motor [17]

Rated torque	*4.4 Nm*
Rated speed	*3000 rpm*
Back EMF	*11.5 V/krpm*
Torque constant	*0.11 Nm/A*
Number of magnetic poles	*8*
Line to line resistance	*0.16 Ω*
Line to line inductance	*0.3 mH*

In the investigated drive system a DC machine is used as the mechanical load of the BLDC motor. The DC machine operates as a generator where permanent magnets are used for the excitation. A variable external resistor is connected in series with the rotor winding to regulate the energy drawn by the machine. Specifications of the generator are shown in Table 4.

Table 4. Specifications of DC machine [18]

V_{dc}	*180 V*
I_{dc}	*11.1 A*
Speed	*3000 rpm*
Torque	*5.1 Nm*
Power	*1600 W*

The power part of the three phase inverter consists of six MOSFETS with antiparallel diodes. The IRFB4410PbF MOSFET has been chosen due to low conduction and switching losses at the operation range of the motor. Detailed characteristic of this MOSFET are shown in Table 5.

Table 5. Main characteristics of IRFB4410PbF.

$_{ds}$	max voltage between drain and source	*00 V*
$_{d}$	max drain current at $T = 100^oC$	*3 A*
$_{ds}$	max resistance between drain and source	*0 mΩ*
$_{r}+t_f$	max rising and falling time delay	*30 ns*

As it is well known, FCs cannot restore energy, but in an EV is quite often that the electric machine operates as a generator. In this case, the reverse diodes of the inverter form a three phase rectifier, which can recover energy to the battery pack. Rotating the machine fast enough will produce voltage higher than *48 V* in the DC bus. When this voltage exceeds *55 V*, the switching technique of the inverter have to change, so that the battery can be charged. The upper side MOSFETs (M1, M3, and M5) are turned off. The lower side MOSFETs (M4, M6, and M2) are simultaneously turned on. The switching of lower side MOSFET and diodes from upper MOSFETs form an interleaved boost converter along with the reactance of the machine's windings. The duty cycle for the lower side MOSFETs is determined by a control loop using the maximum current battery charge as reference.

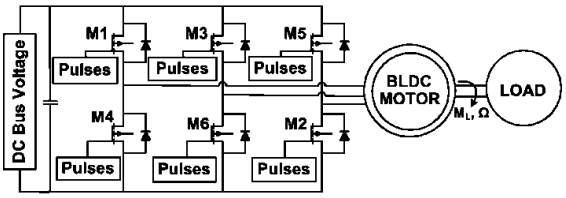

Fig. 4. BLDC motor driven by a three phase inverter.

3. Control Strategy

The energy management between the two electric sources, PEMFC stack and batteries, is based on variations of the former's efficiency as a function of its electric current. This characteristic curve is shown in figure 5.

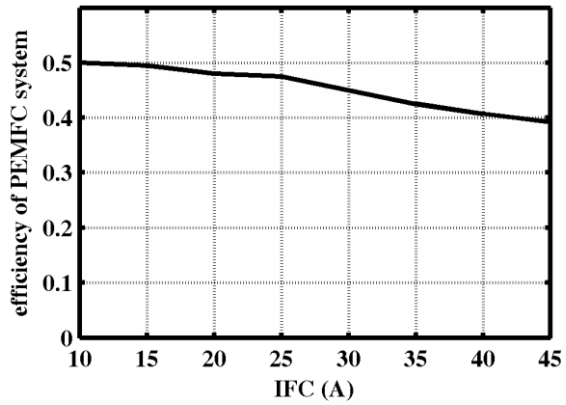

Fig. 5. PEMFC system efficiency curve.

At the rated power (*1200 W – 45 A*) of the PEMFC system the efficiency is 39%. When more power is drawn by the stack the efficiency drops rapidly due to the increasing concentration losses. The control strategy was designed so that the PEMFC's efficiency doesn't become less than 39 %. In specific, when the BLDC motor requires lower than 1200 W, the DC bus voltage is controlled by the interleaved boost converter with a P – I controller.

Battery pack provides additional energy to the BLDC motor, when more than 1200 W are required. In this case, the current produced by the PEMFC stack is limited to its rated value via another P – I controller by measuring the output current of the interleaved boost converter. Also, above 1200 W the DC bus voltage remains constant at 50 V, due to a P – I controller of the bidirectional buck – boost converter.

4. Simulation Results

In this work, the system under investigation has been simulated using MATLAB/SIMULINK software. Two operating scenarios are simulated. In the first, the BLDC motor operates at full load of *1400 W* and both PEMFC stack and batteries provide power to the motor. Some characteristic results are presented in the next figures.

In figure 5, voltage and current produced by the PEMFC stack at *1200 W* are presented. The current ripple of the FC stack at steady state is only *0.4%* and the voltage ripple is less than *0.2%*. These can be accomplished by using a filter in the input of the interleaved boost converter (figure 2).

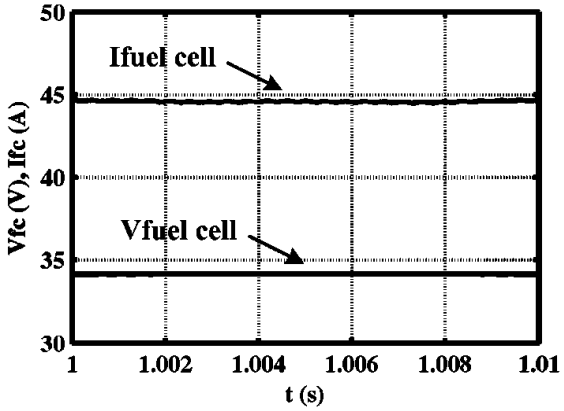

Fig. 6. Voltage and current produced by the FC stack at *1200 W*.

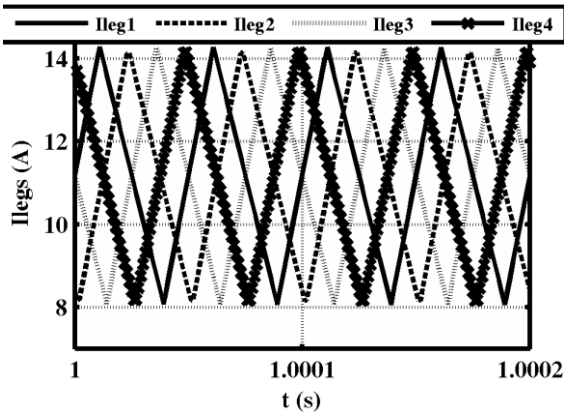

Fig. 7. Input current of the four-leg interleaved boost converter.

The FC current is shared equally to the four legs of the interleaved boost converter as shown in figure 6. The current ripple in each leg is *6.3 A*. By using four legs causes reduced input current ripple to *1.2 A*.

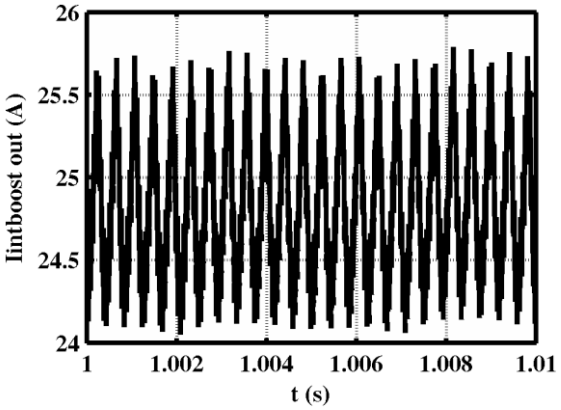

Fig. 8. Output current of the four-leg interleaved boost converter.

Oscillations with frequency six times multiple of the nominal frequency of the motor current are observed. The ripple of electric current is approximately 6%.

In case that the motor requires more than *1200 W*, then battery pack provides the extra energy. In figures 9 and 10 input and output current of the bidirectional buck-boost converter at *200 W* (the remaining power that has to be fed to the motor) are presented respectively.

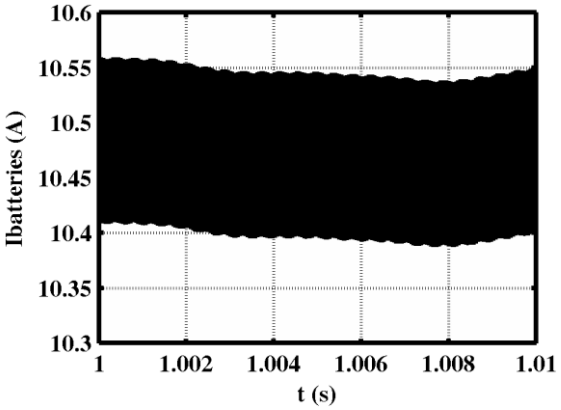

Fig. 9. Input current of the buck-boost converter.

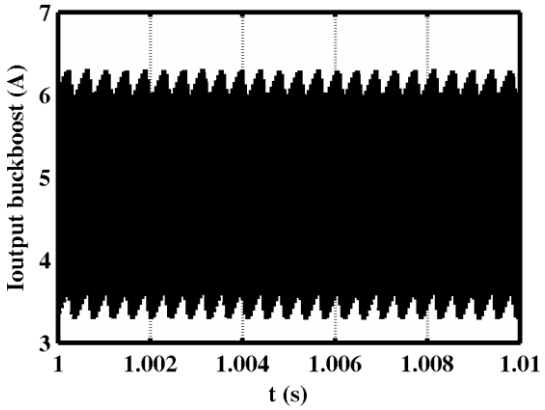

Fig. 10. Output current of the buck-boost converter.

In the output current of the buck-boost converter, oscillation with frequency six times multiple of the nominal value of the motor is observed. The DC bus current and voltage waveforms are shown in figures 11 and 12 respectively. The voltage ripple around the value of *48 V* is less than *0.4%*.

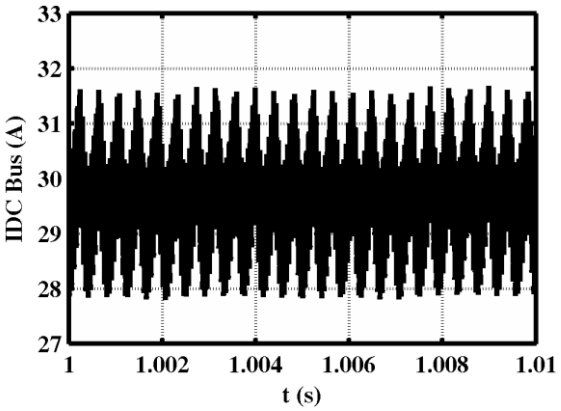

Fig. 11. Current in the DC bus.

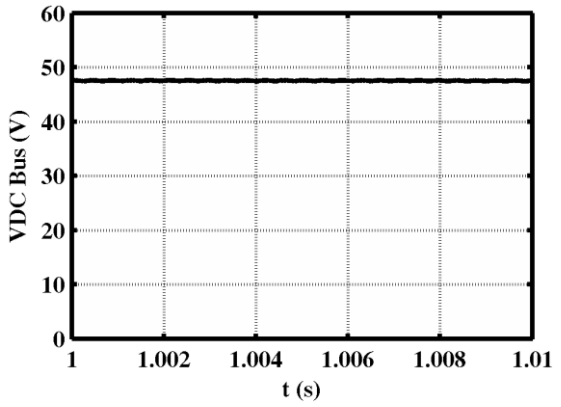

Fig. 12. Voltage in the DC bus.

Phase voltage and line to line voltage of the BLDC motor at the steady state are presented in figures 13 and 14 respectively. The BLDC motor operates at *3000 rpm* by the electric frequency of *200 Hz*. The phase currents of the motor and the electromagnetic torque are presented in figure 15 and figure 16.

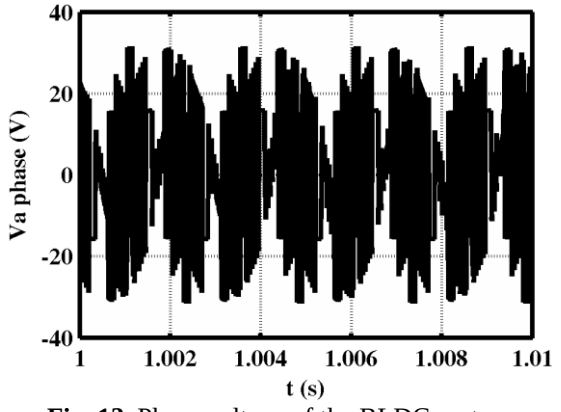

Fig. 13. Phase voltage of the BLDC motor.

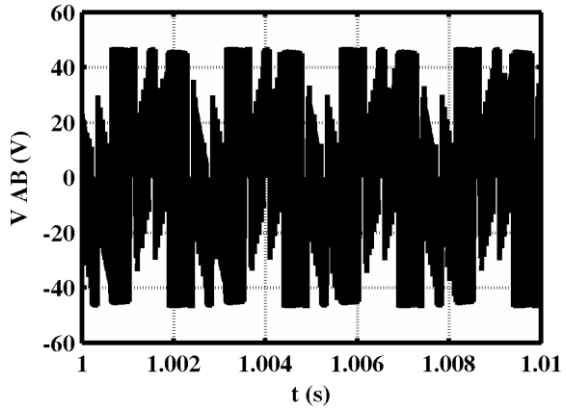

Fig. 14. Line to line voltage of the BLDC motor.

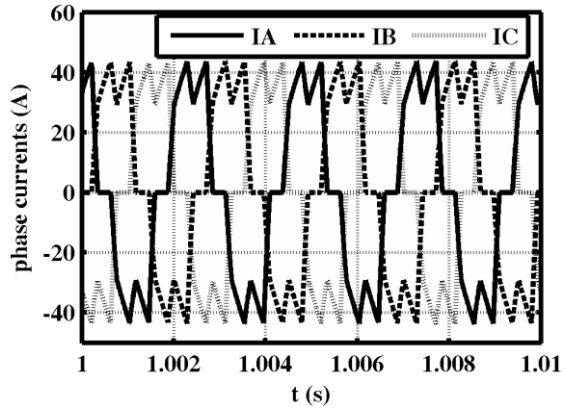

Fig. 15. Phase currents of the BLDC motor.

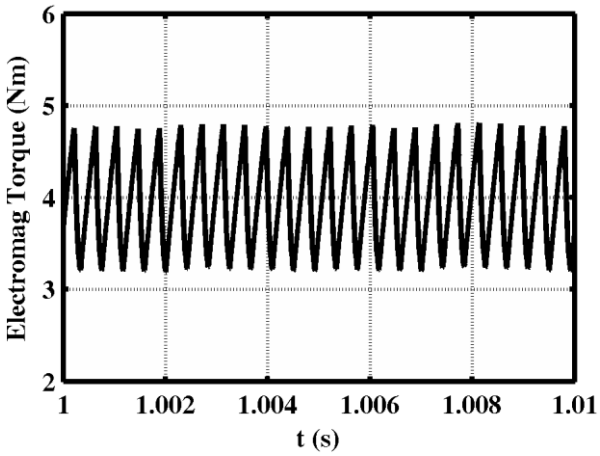

Fig. 16. Electromagnetic Torque of the BLDC motor.

In the second scenario, BLDC machine operates as a generator and the energy is stored to the battery. As the machine rotates with an adequate speed, voltage is produced. Phase and line to line voltages are shown in figure 17 and 18 respectively.

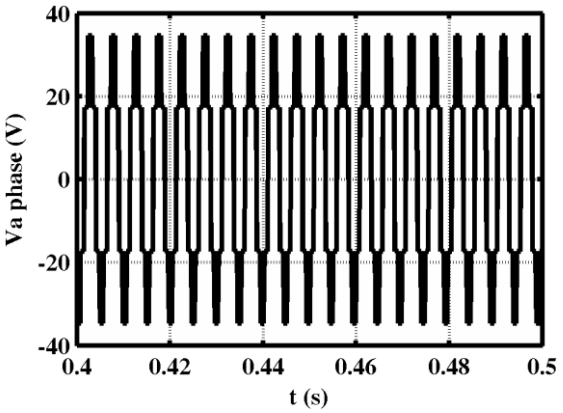

Fig. 17. Phase voltage of the BLDC motor.

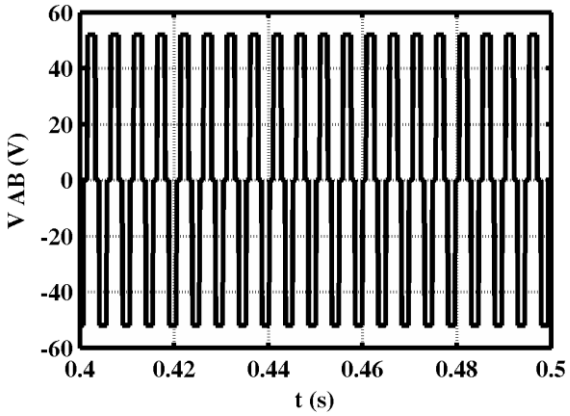

Fig. 18. Line to line voltage of the BLDC motor.

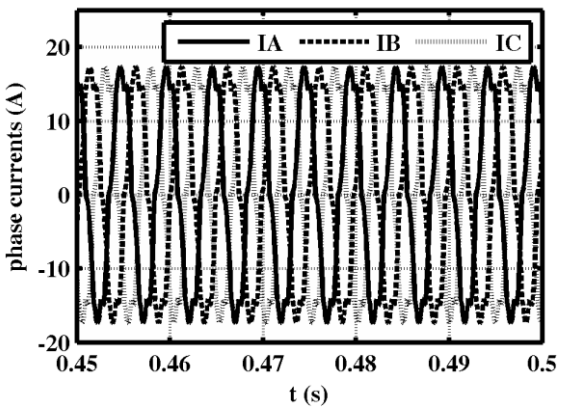

Fig. 19. Phase currents of the BLDC motor.

Now the inverter operates as an interleaved boost converter with three legs that conduct simultaneously. Thus, motor phase currents have almost sinusoidal waveform as shown in figure 19.

The AC voltages are rectified and boosted to *50 V* in the DC bus as shown in figure 20.

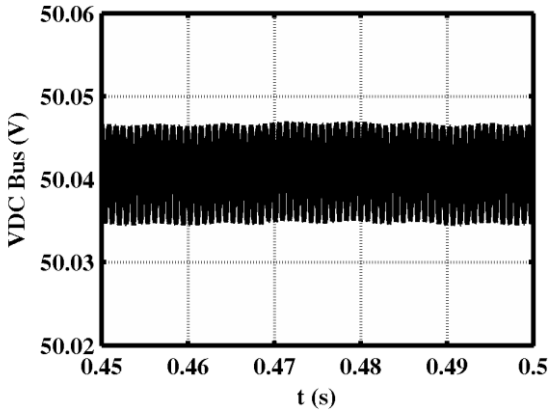

Fig. 20. Voltage in the DC bus.

The current in the DC bus has a negative mean value as shown in figure 21, because energy now flows from the BLDC machine to the battery pack. The current ripple that charges the battery is less than *0.1%* as shown in figure 22.

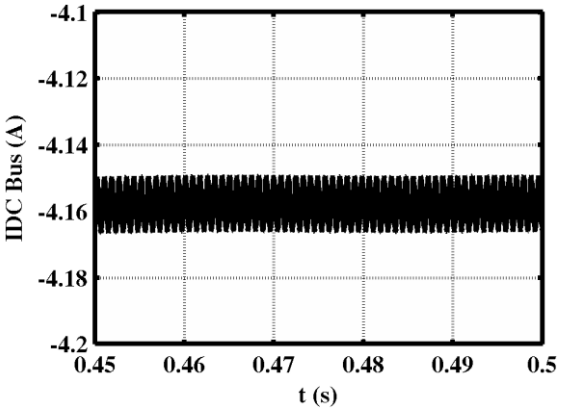

Fig. 21. Current in the DC bus.

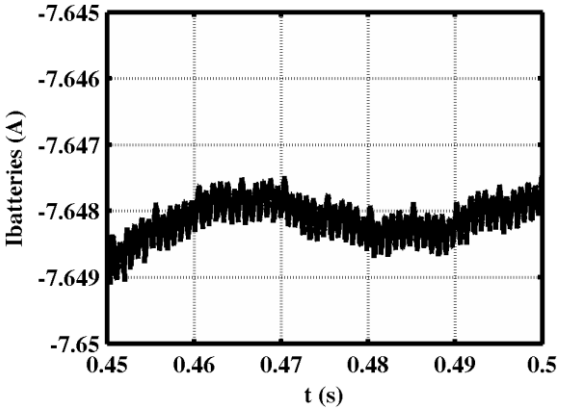

Fig. 22. Current fed to the battery pack.

5. Experimental Results

In order to testify the characteristic curve of V –I produced by this PEMFC system, some experiments have been carried out and the resulted curve is shown in figure 23.

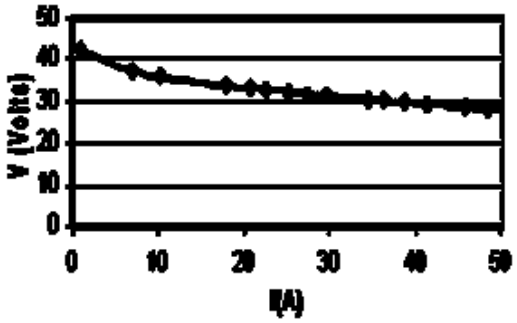

Fig. 23. Experimental characteristic curve *V = f(I)* of the PEMFC system.

It is observed that the output voltage decreases almost linearly to the output current in a wide range up to the nominal electric power. For stack output current is less than *10%* of the nominal value, the output voltage decreases logarithmically according to equation 2, since activation losses are dominant in this operation range.

The interleaved boost converter has been designed and constructed at the laboratory (figure 24). The kind of the conduction mode of each converter, the inductors' value, the number of legs and the switching frequency has been designed in order to decrease the input current ripple. The switching frequency of each leg of interleaved boost converter is *20 kHz*, which leads to input frequency of *80 kHz*.

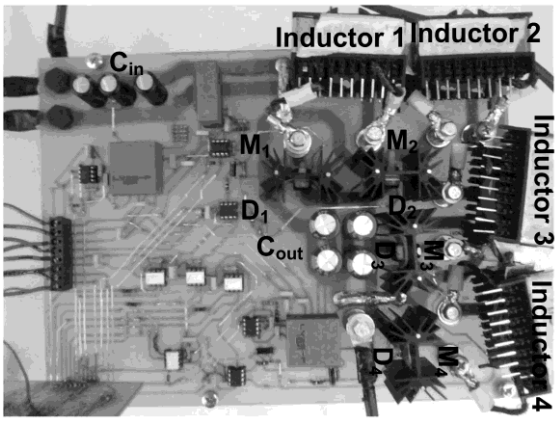

Fig. 24. Laboratory interleaved boost converter.

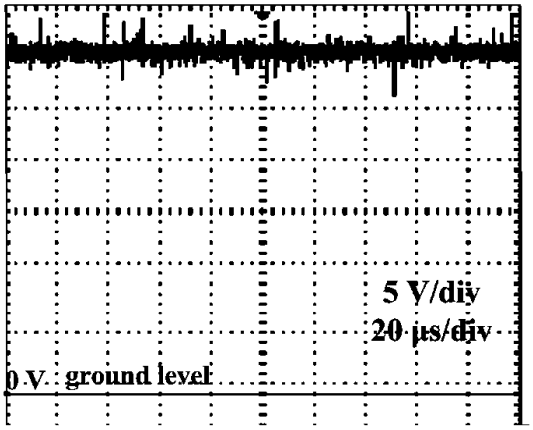

Fig. 25. Input voltage of the four-leg interleaved boost converter.

Figure 25 represents the input voltage of the interleaved boost converter.

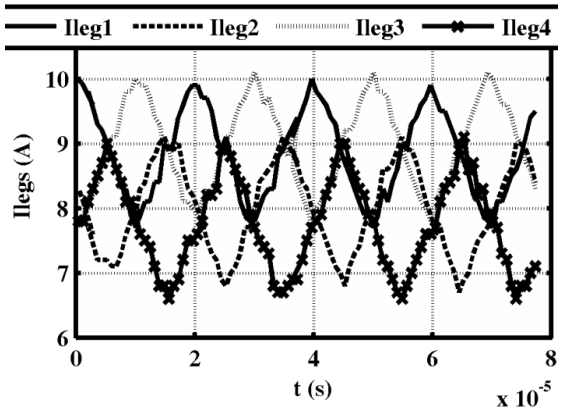

Fig. 26. Input current of the four-leg interleaved boost converter.

Differences in the mean value of each leg current are observed in figure 26. This is because the four inductor values are not identical.

The voltage of the DC bus is *48 V*. Some overshoots occur at turn off of the four power switches.

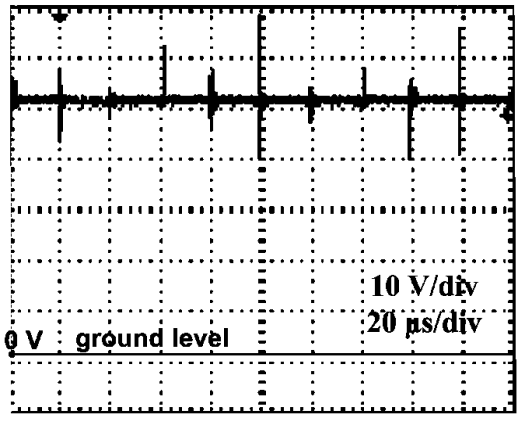

Fig. 27. Voltage in the DC bus.

Figure 28 shows the laboratory experimental system consisting of the BLDC motor driven by the three phase inverter, the load DC generator and measurement devices.

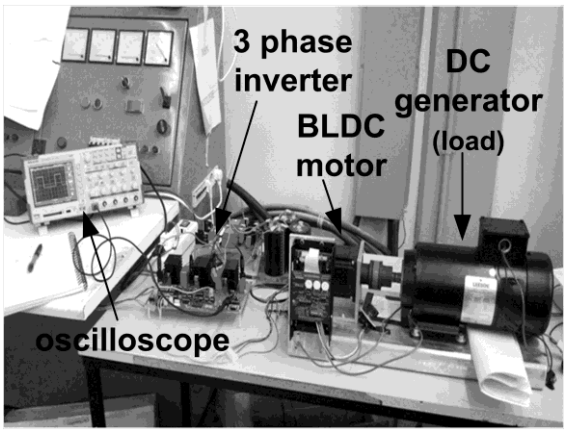

Fig. 28. Photograph of the BLDC motor drive system.

Experiments have carried out at full load (*1400 W*) and at rated speed *3000 rpm*. Line to line voltage and phase currents are presented in figures 29 and 30 respectively. The waveform of the line to line voltage is due to the trapezoidal back EMF that is induced in the stator windings. Also, in figure 30, there are time intervals with duration *T/6*, where phase current is zero. During the commutation in the other two phases overshoot in the phase current occurs at range of *30%*.

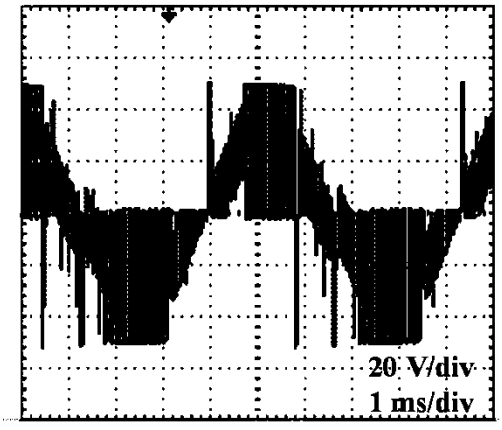

Fig. 29. Line to line voltage of the BLDC motor.

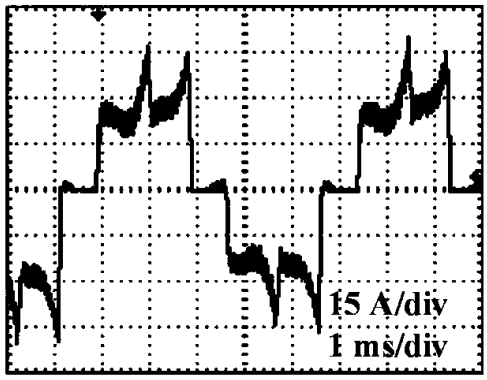

Fig. 30. Phase current of the BLDC motor.

6. Conclusion

In this work a drive system of a FCEV has been designed and simulated using MATLAB/SIMULINK software, where two operating scenarios have been examined. In the first, PEMFC stack and battery pack provide maximum power to the BLDC motor. In the second, the BLDC machine operates as a generator and energy returns to the battery pack. Alternative voltage produced by the BLDC machine is rectified and boosted by changing the modulation technique of the three phase inverter. A bidirectional buck – boost converter downgrades the DC bus voltage to enable charging operation of the battery pack.

A main objective of this work is to design an appropriate structure to manage the energy transfer from the PEMFC stack to the DC bus based on wide high efficiency range. The battery pack is used for reducing the size of the stack and thus the cost as well as regenerative braking can be achieved. The proposed system is considered more advantageous for light EV applications, because of the use of the BLDC motor which has high ratio of power to volume.

Experiments have been carried out to validate the V – I characteristic curve of the PEMFC system and to define its parameters. Also, to testify the behavior of the system at full load of the BLDC motor at steady state some experiments have been done. It was found out that in order to reduce the output current ripple of the PEMFC stack, an interleaved boost converter provides a reasonable solution. So, starvation phenomena of the PEMFC stack are avoided. Moreover, the values of the converters' passive elements and their volume are reduced.

References

[1] Emadi, A.; Young Joo Lee; Rajashekara, K., *"Power Electronics and Motor Drives in Electric, Hybrid Electric, and Plug-In Hybrid Electric Vehicles"*, 2008, IEEE Transactions on Industrial Electronics, Volume 55, Issue 6, pp 2237 - 2245.

[2] Tsotoulidis, S.; Mitronikas, E.; Safacas, A., "Comparative study of three types of step – up DC - DC converters for polymer electrolyte membrane fuel cell applications", International Symposium on Power Electronics Electrical Drives Automation and Motion (SPEEDAM), Pisa – Italy 14 – 16 June 2010, Conference Proceedings.

[3] P. Thounthong, S. Rael, B. Davat, "Control Algorithm of Fuel Cell and Batteries for Distributed Generation System", IEEE Transactions on Energy Conversion, Volume: 23, Issue: 1, March 2008, pp. 148 – 155.

[4] Thounthong, P.; Pierfederici, S.; Davat, B., "Analysis of Differential Flatness-Based Control for a Fuel Cell Hybrid Power Source", 2010, IEEE Transactions on Energy Conversion, Volume 25, Issue 3, pp 909 - 920.

[5] Ying Wu, Hongwei Gao, "Optimization of Fuel Cell and Supercapacitor for Fuel-Cell Electric Vehicles", IEEE Transactions on Vehicular Technology, Volume: 55, Issue: 6, Nov 2006, pp. 1748 – 1755.

[6] P. Garcia, L.M. Fernandez, C.A. Garcia, F. Jurado, "Energy Management System of Fuel-Cell-Battery Hybrid Tramway", IEEE Transactions on Industrial Electronics, Volume: 57, Issue: 12, Dec. 2010, pp. 4013 – 4023.

[7] Lee, J.M.; Cho, B.H., "Power system structure and control strategy for Fuel Cell Hybrid Vehicle", 2008, Power Electronics Specialists Conference, PESC 2008, 15 – 19 June, Rhodes – Greece, Conference Proceedings.

[8] Weiping Xiao, Yunzhi Cheng, Wei-Jen Lee, V. Chen, S. Charoensri, "Hydrogen Filling Station Design for Fuel Cell Vehicles", IEEE Transactions on Industry Applications, Volume: 47, Issue: 1, Jan.-Feb 2011 , pp. 245 – 251.

[9] Caisheng Wang; Nehrir, M.H.; Shaw, S.R., "Dynamic models and model validation for PEM fuel cells using electrical circuits", IEEE Transaction on Energy Conversion, Volume 20, Issue 2, June 2005, pp. 442 – 451.

[10] Ballard, "Nexa™ Power Module User's Manual",2003.

[11] M. Al Sakka, J. Van Mierlo, H. Gualous, P. Lataire, "Comparison of 30KW DC/DC converter topologies interfaces for fuel cell in hybrid electric vehicle", 13th

European Conference on Power Electronics and Applications, EPE '09, 8-10 Sept. 2009, Barcelona – Spain, pp. 1 – 10.

[12] Junhong Zhang, Lai Jih-Sheng, Kim Rae-Young, Wensong Yu, "High-Power Density Design of a Soft-Switching High-Power Bidirectional DC-DC Converter", IEEE Transactions on Power Electronics, ISSN 0885-8993, vol. 22, no.4, 2007, 1145-1153.

[13] H. Plesko, J. Biela, J. Luomi, J.W. Kolar, "Novel Concepts for Integrating the Electric Drive and Auxiliary DC–DC Converter for Hybrid Vehicles", IEEE Transactions on Power Electronics, ISSN 0885-8993, vol. 23, issue 6, 2008, 3025-3034.

[14] A.S. Samosir, A.H.M. Yatim, "Implementation of Dynamic Evolution Control of Bidirectional DC–DC Converter for Interfacing Ultracapacitor Energy Storage to Fuel-Cell System", IEEE Transactions on Industrial Electronics, Volume: 57, Issue: 10, Oct. 2010, pp. 3468 – 3473.

[15] Peter Moreton, "Industrial Brushless Servomotors", Newnes, 2000.

[16] Tsotoulidis, S.; Mitronikas, E.; Safacas, A., "Design of a wavelet multiresolution controller for a fuel cell powered motor drive system", XIX International Conference on Electrical Machines (ICEM), Rome – Italy 6 – 8 September 2010, Conference Proceedings.

[17] Transmotec, "Brushless DC MOTORS, General Catalogue", www.transmotec.com, 13/02/2010.

[18] LEESON, "DC MOTORS", http://www.leeson.com, 13/06/2011.